FDTD Modeling of Antireflection Black Silicon Layers for Solar Cells Applications

Gagik Ayvazyan
National Polytechnic University of Armenia
Yerevan, Armenia
e-mail: agagarm@gmail.com

Karen Ayvazyan
National Polytechnic University of Armenia
Yerevan, Armenia
e-mail: gayvazyan58@mail.ru

Arthur Aghabekyan
National Polytechnic University of Armenia
Yerevan, Armenia
e-mail: aghababarthur@mail.ru

***Abstract*—There is a wide application prospect in black silicon (b-Si), especially in solar cells as an antireflection layer. For further optimization of b-Si, it is important to study its optical characteristics. The relation of structural properties with reflectance and absorption of the b-Si layers by Finite Difference Time Domain method (FDTD) is investigated. A 3D structure is simulated, consisting of cones of different heights, diameters and in-plane periodicities.**

***Keywords*— Modeling, FDTD, solar cell, black silicon.**

I. INTRODUCTION

Black silicon (b-Si) is a nano-structured Si surface formed by a self-organized, maskless process with needle-like surfaces discernible by their black color. The combination of low reflectivity and the semi-conductive properties of Si found in b-Si makes it a prime candidate for application in solar cells as an antireflection layer [1-3].

Modeling the b-Si optical characteristics is useful for finding a relation between the b-Si structural properties and its reflectance spectrum. For this purpose, numerical simulation methods such as the finite differences time-domain method (FDTD), the Fourier modal method (FMM), the rigorous coupled-wave analysis (RCWA) and the finite element method (FEM) have been used [4-6].

The FDTD method is considered to be one of the most accurate and simple rigorous methods to model anti-reflective properties of sub-wavelength structures. The FDTD method makes use of Fourier transform to obtain the frequency solution and, therefore, enable calculation of optical characteristics of electromagnetic radiation when dealing with complex geometries. These optical characteristics include transmission and reflection of light.

There are several commercially available or free software products that make FDTD simulations significantly easier to use, including XF by Remcom, FDTD Solutions by Lumerical, MEEP, OptiFDTD, EM Explorer, FullWave by RSoft Design Group, and an Electromagnetic Template Library. Commercial software often includes a user-friendly GUI and CAD modeling tools for drawing 2D or 3D materials [6].

In this paper, the FDTD method and the commercially available FDTD simulator from Lumerical Solutions, Inc. (Vancouver, Canada) [7] were used to model the optical characteristics of b-Si.

II. MODEL DESCRIPTION

The FDTD method handles any arbitrarily shaped structure naturally using an explicit numerical solution to Maxwell's curl equations. Two and three dimensional Maxwell's equations can be solved by Lumerical FDTD Solutions simulator [7]. It allows the user to input predesigned structures to build complex geometries or the user can create structures using powerful scripting methods, similar to Matlab scripts. The electromagnetic fields $E(r,\lambda)$, $H(r,\lambda)$ are solved as a function of time. Calculation of electromagnetic fields through either linear or non-linear dispersive media is performed with the help of Fourier transforms. The calculated electromagnetic fields are function of either frequency or wavelength, depending upon the simulation setup.

Lumerical FDTD Solutions simulator uses lookup tables of refractive indices of different materials at different wavelengths. User can import refractive indices calculated in another software package. It is also possible to build composite systems and objects with the help of a structure group. An object or group of objects can be replicated in desired directions for setting up a structure group. The advantage of this type of modeling is that the properties of all or specific objects in a given group can easily be edited in a single step.

The Rough Surface module of the Lumerical FDTD Solutions simulator is firstly used to generate a stochastic surface of b-Si. Rough Surface is determined by such values as root mean square (RMS) amplitude, spatial resolution (δ) and correlation length (LC). The RMS amplitude determines the RMS height of the peaks, δ is the average horizontal distance between the local minimum on the surface and the maximum near it, used to describe the density of needles on the surface, LC is used to determine the surface roughnesses: the lower the LC, the stronger a surface fluctuation. The RMS and δ parameters used in the Rough Surface module were extracted from the SEM and AFM images of the b-Si layers and were 0.2 and 0.1 μm, respectively [8]. The value of the correlation length in both directions (LC_X and LC_Y)

was chosen as one tenth of the spatial resolution to ensure sufficient surface roughness.

Fig. 1 shows a b-Si model based on the Rough Surface module of the Lumerical FDTD Solutions simulator. The 3D simulated structure consists of a Si substrate, on which identical cones are periodically repeated along the X- and Y-axes. The structure is defined by its out-of-plane height (h), base diameter (d), and in-plane periodicity (t).

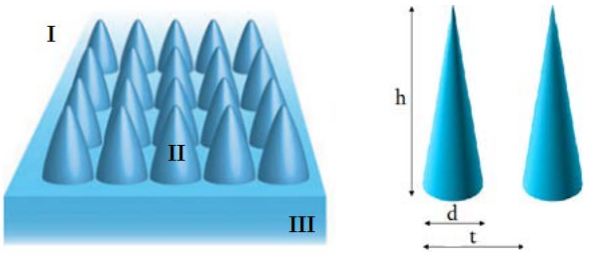

Fig. 1. Schematic diagram of the simulated structure.

Three regions are defined for FDTD simulations, as sketched in Fig. 1. Region I is considered as an air background with a constant refractive index of 1. Region II is the surface textures of b-Si. Region III is the Si substrate. Here, the bottom edge of the simulation area is set inside Region III, so that the reflector exists only between Region I and Region II, thus avoiding the strong oscillations caused by interference between different reflected lights. In order to exclude the influence of Region III on the absorption spectra of b-Si, the thickness of Region III included in the simulation area is set to 1 μm for all the models.

Two frequency-domain field and power monitors are used to calculate the reflectance R and transmission T, respectively. The reflectance monitor is set behind the plane wave source and the transmission monitor is set near the bottom edge of the simulation area. Absorption A is determined according to A=1-R-T.

The modeling was performed at spectral range λ = 300-1000 nm for the following typical parameters of cones: h = 350-900 nm, d = 50-300 nm, t = 100-350 nm. Modeling was conducted for two perpendicular incident light polarizations, and the results were then averaged to obtain a response for unpolarized light. All simulation boundaries were terminated using perfectly matched layer boundary conditions. The Si wafer was assumed as infinitely thick, and the reflections from the polished rear side were not considered.

III. Modeling Results

Fig. 2 shows the 3D dependence of the absorption A on the periodicity t and the height h of the cone at λ = 500 nm. The dependency of the reflection R on the height h of the cone is presented in Fig. 3.

The height h of the cone has a strong influence on the absorption and reflection. With the increase of h, the reflectance decreases significantly, and the absorption increases significantly. We can notice that while the dependence of reflectivity on height is modest in the IR limit (1000 nm), it is significant when observed at lower wavelengths (400-500 nm). The absorption decreases, and the reflectance increases with increasing the periodicity t of the simulated structure. Indeed, the space between the two cones is flat, thus increasing this space leads to a higher reflectance, which tends to the reflectance of a polished Si wafer. Cones have to be as close as possible to achieve very low reflectance values.

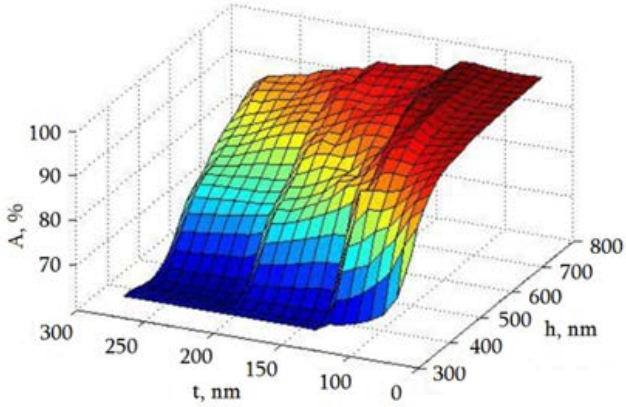

Fig. 2. 3D dependence of the absorption on the periodicity and the height of the cones at λ = 500 nm.

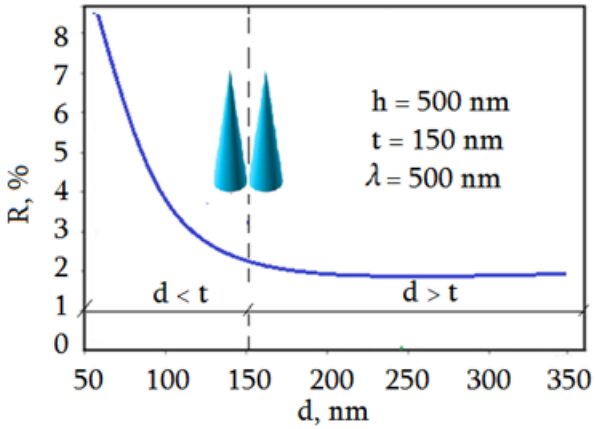

Fig. 3. Cone diameter influence on simulated reflectivity at λ=500 nm.

At constant periodicity, the reflectivity decreases with increasing the cone diameter, while the diameter is lower than the periodicity (d < t, incomplete tiling case). The curve slope decreases from the point where the bases of the structure are in contact (t = d, complete tiling case). The very large decrease in reflectance prior to this point can be understood by the large reduction of the planar surface between the cones. When the cone bases start to overlap (d > t), the reflectivity practically does not change.

Thus, the obtained results can qualitatively be explained by ray tracing technique on the basis of multiple reflections from the surfaces of the cones. Whereas in a planar substrate any reflected light is lost, on a textured substrate the light is redirected to another part of the surface (the so-called “double-bounce” effect). This leads to partial transmission of light into the substrate on two separate cones.

According to [9], we introduce the following ray classification: (a) incident rays; (b) reflected rays formed by incident rays after their reflection from the texture, which revert back into the incident medium after some number of consecutive reflections; (c) refracted rays formed by incident or reflected rays after they get into the texture; and (d) secondary rays formed by refracted rays if they leave the

texture (Fig. 4). Only reflected and secondary rays make contributions to the total reflection $R=R_{refl}+R_{sec}$.

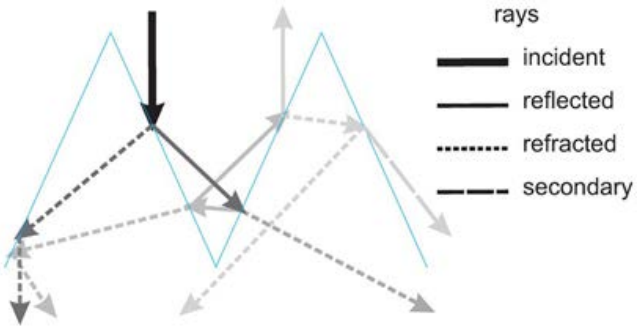

Fig. 4. Rays from two separate cones.

It should be noted that, in addition to multiple reflections, there are two mechanisms for reducing reflection of real b-Si layers [10]:

1. when the size of the texture features is large compared to the wavelength of the solar spectrum, surface scattering is responsible for an elongated light path and enhanced absorption;

2. for sub-100 nm nanostructured Si, the surface feature sizes are so small that the surface essentially acts as an effective index medium and is optically flat. In this case, there is a smooth refractive index transition from air to bulk Si, via the nanostructured surface. Due to the effective refractive index gradient, there is no abrupt interface between Si (n = 3.4) and air (n = 1) and the Fresnel reflections are strongly reduced.

In order to see the light trapping effect via the electric field intensity distribution inside and around the Si cones with different relation h/d, two-dimensional FDTD simulation was carried out. Fig. 5 shows the normalized electric field intensity distributions E(r,λ) at wavelength 500 nm for cones with h = 2d and h = d. It seems that in the latter case, the waves reflected from the surface of the cone, have a greater intensity.

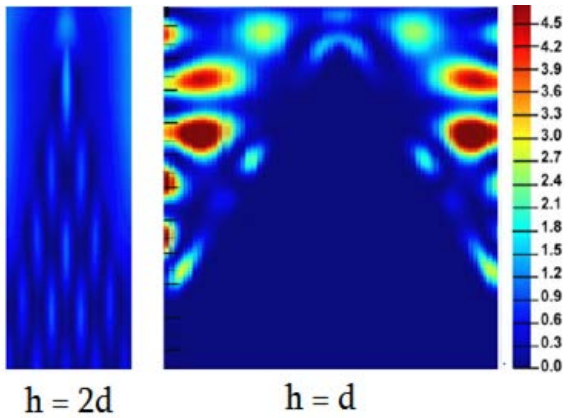

Fig. 5. FDTD simulated electric field intensity distributions E(r,λ) for cones with h=2d and h=d.

The FDTD simulated normalized distributions of the electron-hole pairs generation rate in Si substrate with cone at λ = 400 nm and 1000 nm are presented in Fig. 6. For comparison, the same distributions are shown in non-textured (planar) substrate.

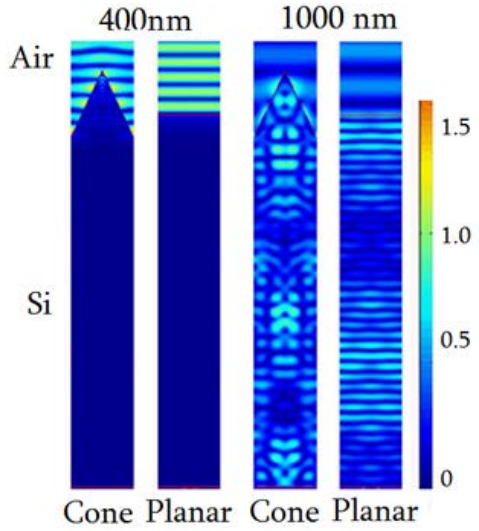

Fig. 6. FDTD simulated normalized distributions of the electron-hole pairs generation rate in Si substrate with and without (planar) cone at λ=400 nm and 100 0nm.

In the case of short waves, the generation of electron-hole pairs takes place mainly in the peripheral layer surrounding the cone. In the case of long waves, the generation takes place in the entire volume of the Si substrate. The presence of cones leads to a noticeable increase in the speed of generation of current carriers.

From a practical point of view, it is also important to model the optical characteristics depending on the angle between the incident beam and the normal surface area of the Si substrate. This property is useful in solar cell applications where a maximum amount of light is required independently of the position of the photovoltaic station with respect to the Sun.

Fig. 7 shows the 3D dependence of the simulated reflectivity R on the incident angle θ_i and wavelength λ. As shown Si substrate with cones exhibits a low reflectivity (below 3%) in the visible range for incidence angles up to 50° from the normal of the surface. But for higher angles, the reflectance increases up to 5% at 60° and even higher than 10 % at 70°. This result shows the potential for improved solar cell performance using b-Si at non-ideal incident angles.

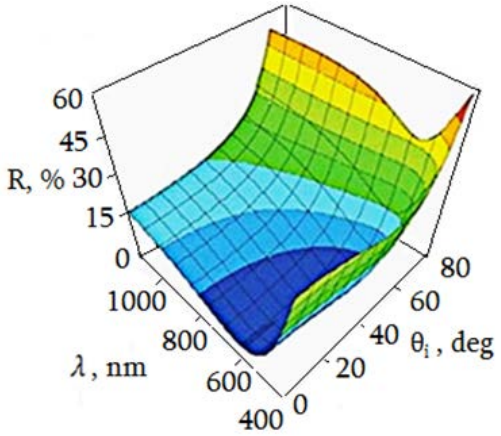

Fig. 7. 3D dependence of the simulated reflectivity on the incident angle and wavelength.

It should be noted that the results of modeling of the reflectance of b-Si are in good agreement with the results of experimental studies [11]. However, because of the computationally limited size of the simulated Si volume and the limited sampled areas of the random surfaces, and since the rear-side surface reflection is disregarded, the numerical simulations predict lower absorptance values than those observed experimentally.

IV. CONCLUSION

The FDTD modeling revealed that b-Si layers effectively suppress reflection in the wavelength range λ = 400–1000 nm. The light-trapping performance primarily depends on the geometry of the needles. With the decrease on periodicity and increase in height of the cone, the reflectance decreases significantly, and the absorption increases significantly. The reflectance stays low even at very high incident angles. This result shows the potential for improved solar cell performance using b-Si at non-ideal incident angles.

ACKNOWLEDGMENT

This work was made possible in part by a research grant from the Yervand Terzian Armenian National Science and Education Fund (ANSEF) based in New York, USA.

REFERENCES

[1] M. Otto, M. Algasinger, H. Branz and B. Gesemann, "Black Silicon Photovoltaics", *Adv. Opt. Mat.*, vol. 3, no 2, pp. 147-164, 2015.

[2] G. Y. Ayvazyan, R. N. Barseghyan and S. A. Minasyan, "Optimization of Surface Reflectance for Silicon Solar Cells", *Green Energy and Smart Grids. E3S Web of Conf.*, vol. 92, pp. 01008-01012, 2018.

[3] Peng Zhang, Yingchun Zhao and Shibin Li, "Review Application of Nanostructured Black Silicon", *Nanoscale Res. Let.*, vol. 13, pp. 1-10, 2018.

[4] F. Atteia, L. Rouzo, L. Denaix, D. Duche, G. Berginc, J. Simon and L. Escoubas, "Morphologies and Optical Properties of Black Silicon by Room Temperature Reactive Ion Etching", *Mat. Res. Bulletin*, vol. 13, pp. 110973 1-9, 2020.

[5] Shijun Ma, Shuang Liu, Qinwei Xu, Junwen Xu, Rongguo Lu, Yong Liu and Zhiyong Zhong, "A Theoretical Study on the Optical Properties of Black Silicon", *AIP Advance*, vol. 8, pp. 035010 1-10, 2018.

[6] K. Han and Chih-Hung Chang, "Numerical Modeling of Sub-Wavelength Anti-Reflective Structures for Solar Module Applications", *Nanomaterials*, vol. 4, pp. 87-128, 2014.

[7] The Lumerical Solutions Inc., Canada website. [Online]. Available: http://www.lumerical.com.

[8] M. V. Katkov, G. Y. Ayvazyan, V. R. Shayapov and M. S. Lebedev, "Modeling of the Optical Properties of Black Silicon Passivated by Thin Films of Metal Oxides", *J. of Contemporary Phys.*, vol. 55, no. 1, pp. 16-22, 2020.

[9] A. Deinega, I. Valuev, B. Potapkin and J. Lozovik, "Minimizing Light Reflection from Dielectric Textured Surfaces", *J. Opt. Soc. Am. A.*, vol. 28, no. 5, pp. 770-776, 2011.

[10] X. Liu,, P. Coxon, M. Peters, B. Hoex, J. Cole and D. Frayc, "Black Silicon: Fabrication Methods, Properties and Solar Energy Applications", *Energy & Env. Sci.*, vol. 7, no. 10, pp. 3223–3263, 2014.

[11] G. Y. Ayvazyan, M. V. Katkov, M. S. Lebedev, V. R. Shayapov, M. Yu. Afonin, D. E. Petukhova, I. V. Yushina, E. A. Maksimovskii and A. V. Aghabekyan, "Anti-Reflection Properties of Black Silicon Coated with Thin Films of Metal Oxides by Atomic Layer Deposition", *J. of Contemporary Phys*., vol. 56, no 3, pp. 240-246, 2021.